Formation of Viscoelastic Wormlike Micellar Solutions in Mixed Nonionic Surfactant Systems

Durga P. Acharya and Hironobu Kunieda*

Graduate School of Environment and Information Sciences, Yokohama National University, 79-7 Tokiwadai, Hodogaya-ku, Yokohama 240-8501, Japan

Received: May 13, 2003; In Final Form: July 9, 2003

The addition of short-EO-chain polyoxyethylene dodecyl ether ($C_{12}EO_n$) surfactants to a dilute solution of polyoxyethylene cholesteryl ether ($ChEO_m$, $m = 10$ and 15) induced unidimensional micellar growth leading to the formation of viscoelastic solutions. The viscoelastic systems show Maxwellian behavior over a wide range of shear frequency and are considered to consist of a transient network of wormlike micelles. With increasing concentration of $C_{12}EO_n$ ($n = 1-4$) at fixed $ChEO_{10}$ concentration in a micellar solution phase, at first a gradual and then a steep increase in zero-shear viscosity (η_o) was observed. The mixing fraction of $C_{12}EO_n$ to increase η_o or induce the micellar growth increases in the following order: $C_{12}EO_1 \approx C_{12}EO_2 < C_{12}EO_3 < C_{12}EO_4$. On increasing m of $ChEO_m$ from 10 to 15 in the $ChEO_m-C_{12}EO_3$ system, a sharp increase in η_o is shifted to relatively higher mixing fraction of $C_{12}EO_3$. These results indicate that the average section area per surfactant in a micelle decreases upon the addition of short-EO-chain $C_{12}EO_n$ and that micelles grow to form long rod micelles. Assuming that the cross-sectional area of each of the amphiphiles at the hydrophobic interface, a_s, is constant (ideal surface mixing), the rod micellar length was calculated as a function of the mixing fraction of $C_{12}EO_n$ in the total amphiphile, X, using the data obtained from experimental results. The calculated results on micellar growth well explained the results of rheological measurements.

Introduction

Surfactant molecules self-assemble to form various microstructures such as spherical micelles, wormlike micelles, and hexagonal liquid crystals. Recently, viscoelastic wormlike micelles have drawn considerable interest in basic research and practical applications. Long-chain cationic surfactants such as hexadecyltrimethylammonium bromide (CTAB)[1−6] and hexadecylpyridinium chloride[7−11] have been reported to form wormlike micelles upon the addition of counterions such as salicylate or bromide ions. Above some critical concentration, called the overlapping concentration, wormlike micelles entangle with each other to form a transient network and exhibit viscoelastic properties[12] analogous to those observed in flexible polymer solutions.

Most of the literature reports the formation of viscoelastic wormlike micelles in cationic systems in the presence of strongly binding counterions. There are some reports on significant micellar growth water−nonionic surfactant systems,[13−15] but a highly viscoelastic solution in a dilute region has not been reported. If we could produce a highly viscoelastic system consisting of wormlike micelles in a nonionic surfactant system, then the relation between the packing constraints of hydrophobic chains and micellar growth would be clarified because the complicated interaction between the counterion and headgroup is not necessary to take into account.

Polyoxyethylene cholesterol surfactants are unique nonionic surfactants in which the segregation tendency between the hydrophilic and hydrophobic groups is very strong compared with that of conventional alkyl ethoxylated surfactants. In fact, they form a liquid crystal in a pure state above their melting temperature,[16] whereas the conventional nonionic becomes a simple liquid above its melting temperature. Long-EO-chain cholesterol surfactants form spherical micelles. Hence, if they are mixed with a lipophilic amphiphile, then a sphere−rod micelle transition will take place and a viscoelastic micellar system can be produced in a dilute region.

In this study, we report the formation of a viscoelastic micellar phase of wormlike micelles in mixed systems of polyoxyethylene cholesteryl ether and short-chain polyoxyethylene alkyl ether-type nonionic surfactants. We also study the effect of composition, surfactant headgroups, and temperature on the rheological behavior of the micellar phase in these nonionic systems. To our knowledge, this is the first report on highly viscoelastic and stiff gels in a nonionic−nonionic surfactant mixture system in an aqueous solution.

Experimental Section

Materials. Polyoxyethylene cholesteryl ether ($ChEO_m$, the number of oxyethylene units $m = 10$ and 15) and polyoxyethylene dodecyl ether ($C_{12}EO_n$, $n = 1-4$), purchased from Nihon Emulsion Co. and Nikko Chemicals Co., respectively, were used as received. The schematic molecular structure of $ChEO_m$ is shown in Scheme 1.

Phase Diagram. For the study of phase behavior, sealed ampules containing required amount of reagents were homogenized and left in a water bath at 25 °C for a few days (for the W_m phase) to several weeks (for the liquid crystal phase) for equilibration. Phases were identified by visual observation and/or small-angle X-ray scattering (SAXS) performed on a small-angle scattering goniometer with a 15-kW Rigaku rotating anode generator (RINT 2500). The samples were covered with plastic films (Mylar seal method) for the measurement.

* Corresponding author. E-mail: kunieda@ynu.ac.jp. Phone and Fax: +81-45-339 4190.

10.1021/jp0353237 CCC: $25.00
Published on Web 08/20/2003

SCHEME 1: Molecular Structure of Polyoxyethylene Cholesteryl Ether

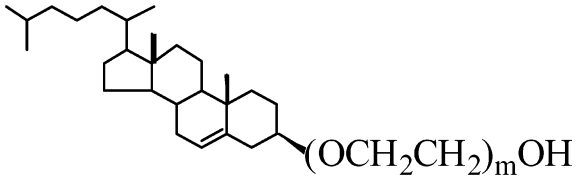

Dynamic Light Scattering (DLS). Dynamic light scattering was performed at 25 °C in a DLS 7000 (Photal, Otsuka Electronics, Japan) equipped with an ALV-5000 multiple-τ digital correlator (ALV-GmbH, Germany) using a He−Ne laser as a light source. The intensity−time correlation function $g_2(t)$ was measured at five different scattering angles: 45, 60, 75, 90, and 110°. For each sample, an apparent diffusion coefficient D_{app} was obtained from an extrapolation of the first cumulant Γ divided by q^2 to zero scattering vector ($q \rightarrow 0$); that is,

$$D_{app} = \lim_{q \rightarrow 0} \Gamma\,(q)\,/q^2$$

The hydrodynamic radius (R_h) was determined using the Stokes−Einstein equation

$$R_h = \frac{kT}{6\pi\eta_s D_{app}}$$

where k is the Boltzmann constant, T is the absolute temperature, and η_s is the viscosity of the solvent (water).

Rheological Measurements. Samples for rheological measurements were prepared by adding the required amount of $C_{12}EO_n$ to a measured volume (5−10 mL) of an aqueous $ChEO_m$ solution of a desired concentration. The samples were homogenized and left in the water bath at 25 °C for at least 48 h to ensure equilibration before performing measurements. Rheological measurements were performed in an ARES7 rheometer (Rheometric Scientific) at 25 °C (unless otherwise stated) using couette (cup diameter, 34 mm; bob diameter, 32 mm; bob length, 33.3 mm) and cone-plate (two sizes: 50- and 25-mm diameters, each having a cone angle of 0.04 rad) geometry depending on the viscosity of the sample. Similar rheological results were found for samples regardless of the type of the geometry chosen in the measurement. Dynamic frequency-sweep measurements were performed in the linear viscoelastic regime of the samples, as determined previously by dynamic strain-sweep measurements.

To understand the effects of the concentration and size of headgroups of the surfactant on rheological properties, steady and oscillatory shear measurements on different series of samples were performed. In each of these series, the concentration of $ChEO_m$ (M) in the total system is fixed, and the concentration of $C_{12}EO_n$ (mole fraction of $C_{12}EO_n$ in the total amphiphile, X) is varied.

Results

1. Phase Behavior. The phase behavior of the $ChEO_{10}$−$C_{12}EO_3$−water system at 25 °C in a water-rich region is shown in Figure 1. Successive additions of $C_{12}EO_3$ to the micellar (W_m) phase of the $ChEO_{10}$−water binary system results in a W_m−hexagonal (H_1) phase−lamellar (L_α) phase transition at higher $ChEO_{10}$ concentration, whereas a W_m−L_α phase transition is observed at lower $ChEO_{10}$ concentration and is attributed to the decrease in surfactant layer curvature with the incorporation

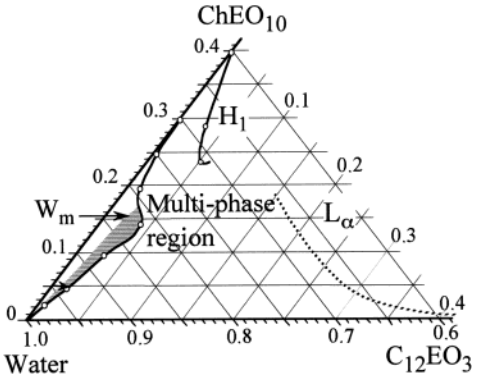

Figure 1. Partial phase diagram of the $ChEO_{10}$−$C_{12}EO_3$−water system in the dilute region at 25 °C. H_1 and L_α are the hexagonal and lamellar liquid-crystal phases, and W_m is the micellar phase. The region of high viscosity within the W_m phase is tentatively shown by the shaded area.

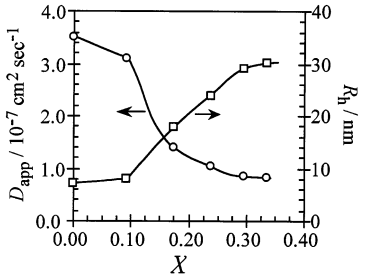

Figure 2. Variation of the apparent diffusion coefficient, D_{app} (○) and hydrodynamic radius R_h (□) of aggregates in the 0.03 M $ChEO_{10}$−$C_{12}EO_3$ system as a function of the mole fraction of $C_{12}EO_3$ (X) at 25 °C. The solid lines are aids to the eyes.

of $C_{12}EO_3$ into the palisade layer of the surfactant aggregate. Inside the W_m phase region, there is a region, shown tentatively by the shaded area in the phase diagram (Figure 1), where the samples have very high viscosity and are even transparent and gel-like in the high surfactant concentration region near the phase boundary. These highly viscous samples are optically isotropic when still but show shear birefringence. The shaded region of the highly viscous micellar phase appears to be extended from the protruded part of the H_1 phase toward the water corner, but to be exact, the shaded area is nearly parallel to the water−surfactant axis. At higher mixing fractions of $C_{12}EO_3$, phase separation takes place, and vesicular dispersion was observed in the multiphase region. Hence, finally, the surfactant layer curvature becomes flat or zero at high $C_{12}EO_3$ content.

2. Dynamic Light Scattering. Dynamic light scattering was performed in a series of samples by keeping the concentration of $ChEO_{10}$ fixed (0.03 M ≈ 2.5 wt %) and varying the mixing fraction of $C_{12}EO_3$. The plot of the apparent diffusion constant (D_{app}) and hydrodynamic radius (R_h) as a function of the mole fraction (X) of $C_{12}EO_3$ in the total amphiphile in the system is shown in Figure 2. In the aqueous $ChEO_{10}$ solution, the measured value of R_h is 7.0 nm. Considering the length of the lipophilic (cholesteric) part of the $ChEO_{10}$ amphiphile to be 1.85 nm[16] and the average length of an oxyethylene unit in a meander configuration to be 0.20 nm,[17] as reported previously, the radius of the aggregate becomes ∼3.85 nm if we assume the aggregate to be spherical. A much higher experimental value of R_h (∼7.0 nm) suggests a nonspherical, most probably short rod shape of the aggregate of $ChEO_{10}$ in the W_m phase of the water−surfactant binary system. However, a similar measurement gave a smaller value of R_h (6.1 nm) for $ChEO_{15}$ micelles in a 0.03 M (∼3 wt %) $ChEO_{15}$ solution. Assuming a spherical shape of the $ChEO_{15}$ aggregates, the radius of the aggregates is expected to be ∼4.85 nm, which is closer to the R_h value. Hence, this

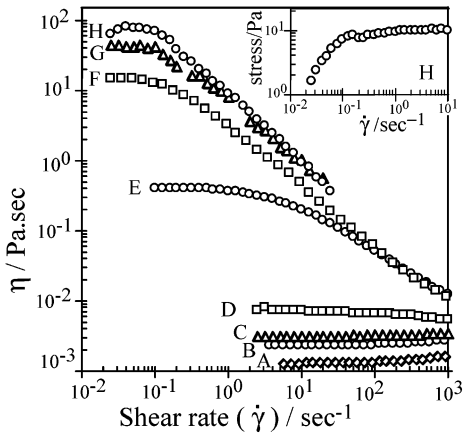

Figure 3. Steady shear-rate−viscosity plots of the micellar solution of 0.06 M $ChEO_{10}$−$C_{12}EO_3$ systems at various mole fractions of $C_{12}EO_3$ (X): (A) 0, (B) 0.09, (C) 0.14, (D) 0.17, (E) 0.24, (F) 0.29, (G) 0.36, and (H) 0.42. Inset: variation of shear stress against shear rate for system H ($X = 0.42$).

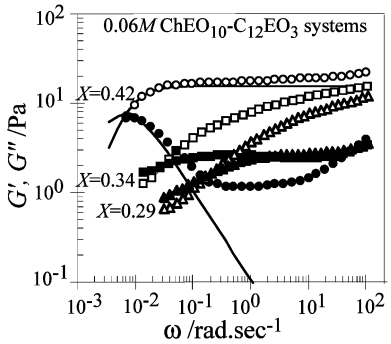

Figure 4. Variation of storage modulus G' (open symbols) and loss modulus G'' (filled symbols) as a function of oscillatory shear frequency (ω) in 0.06 M $ChEO_{10}$−$C_{12}EO_3$ systems at various mole fractions of $C_{12}EO_3$ (X). The solid lines represent the Maxwell fittings for the system with $X \approx 0.42$.

suggests that $ChEO_{15}$ micelles have a less elongated shape, which may be attributed to the larger headgroup of $ChEO_{15}$ or a larger cross-sectional area of the headgroup at the hydrophobic interface, a_s. In fact, it is known that a_s monotonically increases with increasing EO chain length.[18]

Successive additions of $C_{12}EO_3$ to aqueous $ChEO_{10}$ solution result in a small amount of micellar growth at the beginning, followed by rapid unidimensional micellar growth, as indicated by the plots of D_{app} and R_h with $C_{12}EO_3$ concentration (Figure 2). Above $X \approx 0.2$, however, D_{app} starts decreasing slowly, followed by a nearly constant minimum value that corresponds to the beginning of the overlapping of wormlike micelles. Under this condition, hydrodynamic interaction between wormlike micelles begins, and R_h becomes identical to the hydrodynamic correlation length.[19,20] In agreement with the DLS result, the results of rheological measurements of 0.03 M $ChEO_{10}$−$C_{12}EO_3$ systems, which will be discussed later (Figure 5), also show that the viscosity starts to increase rapidly at $X \approx 0.2$.

3. Rheological Study. In this section, we first discuss the effect of the concentration of $C_{12}EO_3$ on the rheology of 0.06 M (≈5 wt %) $ChEO_{10}$−$C_{12}EO_3$ systems. It will be followed by the discussion of the effect of the concentration of $ChEO_{10}$ on the rheology in $ChEO_{10}$−$C_{12}EO_3$ systems. In the next step, we will show the effect of size on the surfactant headgroup by considering the rheology of 0.06 M $ChEO_{10}$−$C_{12}EO_n$ ($n = 1$, 2, and 4) systems and then 0.06 M $ChEO_{15}$−$C_{12}EO_3$ systems.

Effect of $C_{12}EO_3$ Concentration in 0.06 M $ChEO_{10}$−$C_{12}EO_3$ Systems. Steady-state shear-rate viscosity plots for the aqueous 0.06 M $ChEO_{10}$−$C_{12}EO_3$ systems at various concentration of $C_{12}EO_3$ are shown in Figure 3. At low $C_{12}EO_3$ mixing fraction (up to $X \approx 0.17$), the viscosity is very low and is independent of shear at low shear rate (Newtonian fluid), but there is a small increase in viscosity with shear at high shear rate, probably because of shear-induced collisions between the initially short micelles leading to micellar growth beyond the equilibrium size.[21] At $X \approx 0.24$ and above, however, the Newtonian behavior is limited to low shear rate, and viscosity decreases monotonically with increasing shear rate, which can be taken as evidence of the formation of long wormlike micelles. At high $C_{12}EO_3$ concentration ($X \approx 0.36$ and above), samples are gel-like with very high viscoelasticity and show an apparent yield stress that is typical of gel at low shear rates,[22] as shown in the inset of Figure 3.

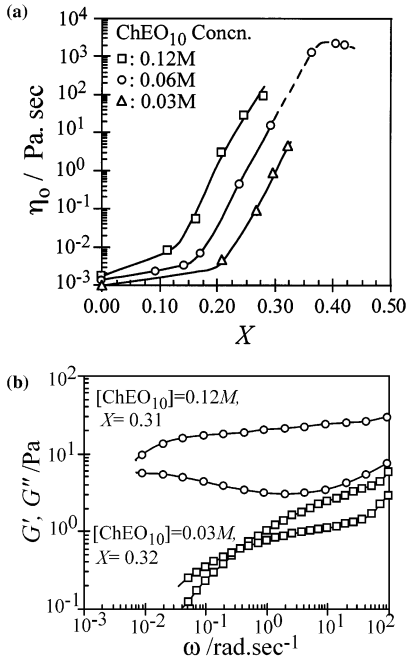

Figure 5. (a) Variation of zero-shear viscosity (η_o) with the mole fraction of $C_{12}EO_3$, X, at various concentrations of $ChEO_{10}$ in aqueous $ChEO_{10}$−$C_{12}EO_3$ systems. (b) Variation of G' (open symbols) and G'' (filled symbols) as a function of ω in 0.03 M $ChEO_{10}$−$C_{12}EO_3$ and 0.12 M $ChEO_{10}$−$C_{12}EO_3$ systems.

To study the viscoelastic properties of the wormlike micellar solution, oscillatory shear measurements have been performed. Figure 4 show the variation of the elastic or storage modulus (G') and the viscous or loss modulus (G'') with oscillation frequency (ω) at $C_{12}EO_3$ concentrations of $X \approx 0.29$−0.42. In these systems, liquidlike behavior ($G' < G''$) is observed in the low-frequency region, but both G' and G'' increase with ω and viscoelastic behavior ($G' > G''$) is observed in the high-frequency region. As can be seen from Figure 4, with increasing concentration of $C_{12}EO_3$ the region of $G' > G''$ extends to lower frequency, and above $X \approx 0.36$ of $C_{12}EO_3$, the system is viscoelastic in a wide range of shear frequency and has a rheological pattern typical of entangled wormlike micelles, as shown in Figure 4 (at $X \approx 0.42$).

The viscoelastic behavior of the entangled micelles is described by the Cates model,[19,23] which considers two processes of stress relaxation—reptation or the reptile-like motion of the micelle along a tube and the reversible scission of micelles—taking place on two time scales, namely, the reptation time τ_{rep} and the breaking time τ_b. The viscoelastic behavior of such a system at low shear frequency often follows the Maxwell model of viscoelastic fluids with a single relaxation time τ given by

$(\tau_b.\tau_{rep})^{1/2}$ and plateau modulus (G_o) described by eqs 1 and 2.[24]

$$G'(\omega) = \frac{\omega^2\tau^2}{1+\omega^2\tau^2}G_0 \quad (1)$$

$$G''(\omega) = \frac{\omega\tau}{1+\omega^2\tau^2}G_0 \quad (2)$$

The rheology of wormlike micelles deviates from Maxwellian behavior at high frequencies, showing an upturn in G''. This deviation arises from the transition of the relaxation mode from "slower" reptation to "faster" Rouse modes.

For the system described by Figure 4 ($X \approx 0.42$), the experimental data are not available in frequency regions below the $G'-G''$crossover frequency (ω_R); the measurements were not carried out in this region because of very long measurement time and, consequently, because of possible changes in sample composition by the evaporation of water. Still, we can estimate G'' at ω_R (G''_{max}) and the relaxation time, τ ($= 1/\omega_R$) for this system. This allows us to estimate G_0 ($\cong 2G''_{max}$) and predict the Maxwell curves (shown by the solid line in Figure 4 for $X \approx 0.42$) over a wide range of frequency. It can be seen in Figure 4 that with increasing the concentration of $C_{12}EO_3$ G' develops to a well-defined plateau value ($G_0 \approx 14.8$ at $X \approx 0.42$) at $\omega > \omega_R$ and also the minima of G'' decreases, which implies that the degree of entanglement of wormlike micelles forming a transient network increases and that the rheology approaches Maxwellian behavior. At $\omega > 0.2$ rad s^{-1}, G'' shows a wide minimum followed by an upturn with increasing ω, suggesting a wide spectrum of stress relaxation at high frequency.

Effect of $ChEO_{10}$ Concentration in $ChEO_{10}-C_{12}EO_3$ Systems. Figure 5a shows the zero-shear viscosity (η_o) as a function of mole fraction (X) of $C_{12}EO_3$ in the total amphiphile at different $ChEO_{10}$ concentration, viz., 0.03, 0.06, and 0.12 M. The η_o values for the Newtonian systems of low viscosity have been determined by extrapolating the viscosity to zero-shear rate. For viscoelastic systems following Maxwellian behavior at low-shear frequency, η_o values were estimated from the following equation:[24]

$$\eta_o = G_0\tau \quad (3)$$

The η_o values of gel-like samples obtained from the estimated values of G_0 and τ are only the approximate values and are shown by dotted lines. It can be seen in this Figure that η_o increases at approximately a similar rate with increasing X for each of these series. At any value of X, η_o is higher for the systems with higher $ChEO_{10}$ concentrations. The results of oscillatory shear measurements of 0.03 M $ChEO_{10}-C_{12}EO_3$ and 0.12 M $ChEO_{10}-C_{12}EO_3$ systems at roughly similar mixing fractions of $C_{12}EO_3$ (X) are shown in Figure 5b. From this Figure, it can be seen that on increasing the concentration of $ChEO_{10}$ (at fixed X) the system shows a large increase in both G' and G'', with $G' > G''$ (viscoelastic behavior) in wide range of ω (0.01−100 rad s^{-1}). In 0.12 M $ChEO_{10}-C_{12}EO_3$ systems, at a high mixing fraction of $C_{12}EO_3$ ($X \approx 0.28-0.40$), similar (gel-like) behavior is observed. The sharp increase in η_o and viscoelasticity with increasing $ChEO_{10}$ concentration is attributed to a small effective cross-sectional area of $ChEO_{10}$ at high concentration, as described later.

Effect of the Headgroup Size of Surfactants. To study the effect of the headgroup size of surfactants on rheological behavior, steady-state shear and oscillatory measurements were performed on samples of 0.06 M $ChEO_{10}-C_{12}EO_n$ with different

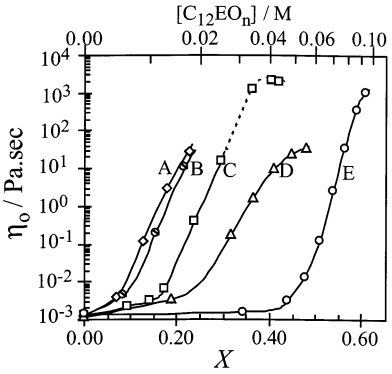

Figure 6. Variation of zero-shear viscosity (η_o) with mixing fraction of $ChEO_n$ (X) in different 0.06 M $ChEO_{10}-ChEO_n$ systems—(A) $C_{12}EO_1$, (B) $C_{12}EO_2$, (C) $C_{12}EO_3$, (D) $C_{12}EO_4$—and (E) 0.06 M $ChEO_{15}-C_{12}EO_3$.

EO chain lengths ($n = 1$, 2, and 4) and 0.06 M $ChEO_{15}-C_{12}EO_3$ systems. The steady shear-rate viscosity plots (not shown here) show similar trends to those observed in 0.06 M $ChEO_{10}-C_{12}EO_3$ systems (Figure 3), that is, Newtonian behavior at low $C_{12}EO_n$ concentrations and shear thinning at higher $C_{12}EO_n$ concentrations. The variation of zero-shear viscosity (η_o) with the concentration of $C_{12}EO_n$ ($n = 1-4$) in 0.06 M $ChEO_{10}-C_{12}EO_n$ and 0.06 M $ChEO_{15}-C_{12}EO_3$ systems is shown in Figure 6. Although gel-like samples were also observed in $ChEO_{10}-C_{12}EO_1$ and $-C_{12}EO_2$ systems at higher concentrations of $C_{12}EO_1$ and $C_{12}EO_2$, the $G'-G''$ crossover frequencies were very low (much lower than 0.01 rad s^{-1}) and were not measured. Therefore, η_o could not be estimated for these samples. However, in $ChEO_{10}-C_{12}EO_4$ systems, no gel-like samples were observed over the whole mixing range before phase separation. Figure 6 shows that in $ChEO_{10}-C_{12}EO_n$ systems with decreasing headgroup size (smaller n) and a sharp increase in η_o the overlapping of wormlike micelles begins at lower $C_{12}EO_n$ concentration and micellar growth occurs more rapidly, as indicated by the increasing steepness of η_o-concentration curves. Judging from these observations, the ability of $C_{12}EO_n$ to induce micellar growth in $ChEO_{10}-C_{12}EO_n$ systems follows the order $C_{12}EO_1 \approx C_{12}EO_2 > C_{12}EO_3 \gg C_{12}EO_4$. When the EO chain length (m) of $ChEO_m$ is increased from $m = 10$ to 15, that is, in $ChEO_{15}-C_{12}EO_3$ systems, a sharp increase in η_o begins at a $C_{12}EO_3$ concentration that is much higher than the corresponding concentration in $ChEO_{10}-C_{12}EO_n$ systems (Figure 6). However, once the η_o begins to increase in the $ChEO_{15}-C_{12}EO_3$ system, growth takes place rapidly, and η_o reaches a high value (>1000 Pa s) that is comparable to that of the $ChEO_{10}-C_{12}EO_3$ system, as shown by Figure 6.

Figures 7−9 show the results of oscillatory-shear measurements of different $ChEO_m-C_{12}EO_n$ systems. Figure 7a shows the plot of G', G'' as a function of ω for a 0.06 M $ChEO_{10}-C_{12}EO_4$ system at different $C_{12}EO_4$ concentrations (X). With increasing $C_{12}EO_4$ concentration, the plateau value of G' increases and becomes well defined, and a depression in G'' becomes more pronounced. At $X \approx 0.48$ (circles in Figure 7a), which corresponds to the maximum viscosity region, G_0 (~21 Pa) and G''_{min} are higher than the corresponding values for the viscoelastic 0.06 M $ChEO_{10}-C_{12}EO_3$ system in the maximum viscosity region. Because G_0 is related to the average length between entanglements, l_e, in the network by the equation[7] $G_o \approx kT/l_e^{9/5}$, a larger value of G_o in the 0.06 M $ChEO_{10}-C_{12}EO_4$ system corresponds to a smaller l_e (~82% of l_e in 0.06 M $ChEO_{10}-C_{12}EO_3$), that is, a smaller mesh size of the transient network that is probably due to a higher total surfactant content in the system. However, the crossover frequency in $ChEO_{10}-$

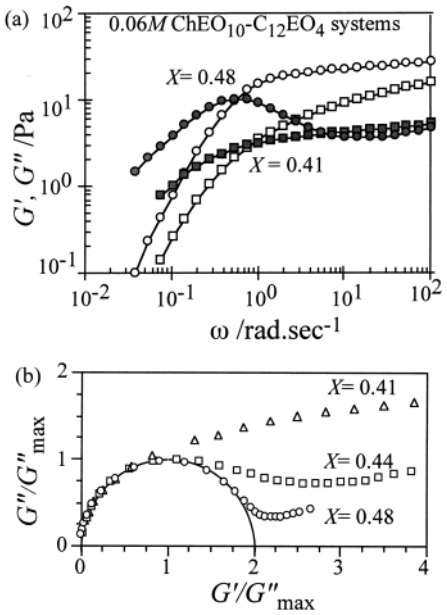

Figure 7. (a) Variation of G' (open symbols) and G'' (filled symbols) as a function of ω in 0.06 M $ChEO_{10}-C_{12}EO_4$ systems at various mole fractions of $C_{12}EO_4$, X. (b) Normalized Cole−Cole plot for 0.06 M $ChEO_{10}-C_{12}EO_4$ systems at different X's.

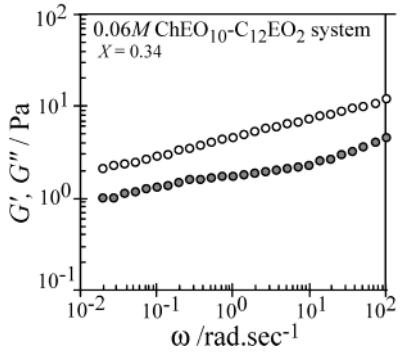

Figure 8. Variation of G' (open symbols) and G'' (filled symbols) as a function of ω in a 0.06 M $ChEO_{10}-C_{12}EO_2$ system at $X = 0.34$.

$C_{12}EO_4$ is much higher than in the $ChEO_{10}-C_{12}EO_3$ system, which corresponds to a shorter τ (~1.8 s in $X \approx 0.48$ $C_{12}EO_4$) or faster stress relaxation. Similarly, it can be seen that the ratio G''_{min}/G_o in the $ChEO_{10}-C_{12}EO_4$ system (~0.18) is higher than in the $ChEO_{10}-C_{12}EO_3$ system (~0.08) in the maximum viscosity region. Because the quantity G''_{min}/G_o is related to the micellar contour length $\bar{L}$ through the following equation when τ_b is much longer than the Rouse time, (τ_R)[8,23]

$$\frac{G''_{min}}{G_o} \approx \frac{l_e}{\bar{L}} \tag{4}$$

the larger G''_{min}/G_o and smaller l_e in $ChEO_{10}-C_{12}EO_4$ suggest a significantly smaller $\bar{L}$ (about $^1/_3$ of the average length in the $ChEO_{10}-C_{12}EO_3$ system). From simple consideration and also on the basis of the Doi−Edward relation[25] ($\tau_{rep} \propto \bar{L}^3 \phi^{3/2}$, ϕ being the volume fraction of surfactant) between the reptation time (τ_{rep}) with $\bar{L}$, it can be expected that the micelles with shorter contour lengths require shorter times to reptate and therefore can undergo stress relaxation quickly (shorter τ). Once again, the Doi−Edward equation[25] that relates the plateau modulus G_o to micellar length via the equation $G_o \propto \phi^{3/2}/\bar{L}$, predicts an increase in G_o with a decrease in $\bar{L}$, probably because a decrease in $\bar{L}$ at a value of ϕ would increase the number of micelles and consequently the number density of micelles in the system. These predictions are consistent with the rheological results of the $ChEO_{10}-C_{12}EO_4$ and $ChEO_{10}-C_{12}EO_3$ systems in maximum viscosity regions. These results indicate that upon decreasing the EO chain length of $C_{12}EO_n$ in the $ChEO_{10}-C_{12}EO_n$ system the average micellar length increases or micellar growth is favored.

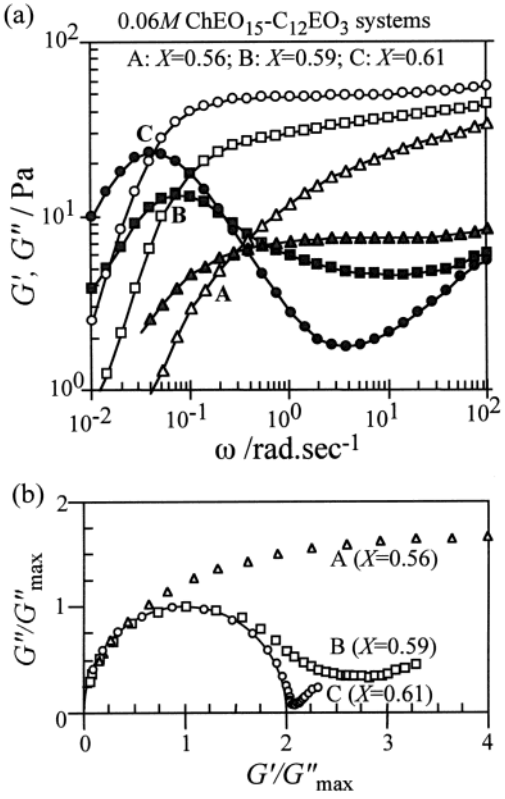

Figure 9. (a) Variation of G' (open symbols) and G'' (filled symbols) as a function of ω in 0.06 M $ChEO_{15}-C_{12}EO_3$ systems at various mixing fractions of $C_{12}EO_3$, X. (b) Normalized Cole−Cole plot for these systems.

Plots of G''/G''_{max} against G'/G''_{max} for 0.06 M $ChEO_{10}-C_{12}EO_4$ systems at different $C_{12}EO_4$ concentrations (including systems not shown in Figure 7a) are shown in Figure 7b. In this plot, known as a normalized Cole−Cole plot,[26] a Maxwell material is characterized by a semicircle centered at $G'(\omega)/G''_{max} = 1$. It can be seen from this Figure that with increasing $C_{12}EO_4$ concentration the system approaches Maxwellian behavior.

Also, in 0.06 M $ChEO_{10}-C_{12}EO_2$ systems, viscoelasticity increases sharply with $C_{12}EO_2$ concentration. However, no clear minima of G'' were observed in the high-frequency region, indicating a wide spectrum of relaxation mechanism. At high concentrations of $C_{12}EO_2$ (within the W_m phase), a gel-type dynamic rheology with $G' > G''$ over a wide range of ω (100−0.01 rad s^{-1}) as shown in Figure 8 is observed. Keeping in mind the relation between the EO chain length and the length of micelles, the formation of highly viscoelastic gels in $ChEO_{10}-C_{12}EO_2$ systems may be associated with the formation of very long micelles that entangle to form an interwoven network. Similar growth in viscoelastic properties is observed in 0.06 M $ChEO_{10}-C_{12}EO_1$ system (data not shown). However, the results are consistent.

The oscillatory shear measurements of 0.06 M $ChEO_{15}-C_{12}EO_3$ systems at various concentrations of $C_{12}EO_3$ are shown in Figure 9a. With increasing concentration of $C_{12}EO_3$, the maximum of the G' value increases, leading to a well-defined plateau modulus (G_o), and G''_{min} in a high-frequency region also

becomes well-defined and deeper, followed by an upturn that is associated with a Rouse mode of stress relaxation.[7] Moreover, the relaxation time τ lengthens as the concentration of $C_{12}EO_3$ increases ($\tau \approx 22$ s at $X \approx 0.61$). G_o (~48 Pa) for the system is 3 times higher than the value observed in 0.06 M $ChEO_{10}-C_{12}EO_3$ systems and corresponds to a smaller mesh size in the transient network in the $ChEO_{15}$ system.

The oscillatory shear behavior observed in the $ChEO_{15}-C_{12}EO_3$ systems, especially at higher $C_{12}EO_3$ concentrations, is typical of entangled wormlike micelles.[19,23] A Cole−Cole plot (Figure 9b) for these systems in the region of high $C_{12}EO_3$ concentration ($X \approx 0.59-0.61$) shows that with an increase in $C_{12}EO_3$ concentration a semicircle is developed with a well-defined dip at a high G'/G''_{max} value, and up to a frequency as high as ~3 rad s^{-1}, the system shows Maxwellian behavior characterized by a single stress-relaxation process (reptation of the micelle along its own contour through the entanglement). The ω corresponding to the minimum of G''/G''_{max} in the high-frequency region is approximately equal to the inverse of the average time of the breaking (τ_b) of the wormlike micelle. For the $ChEO_{15}-C_{12}EO_3$ system at $X \approx 0.61$, the estimated value of τ_b is ~0.6 s.

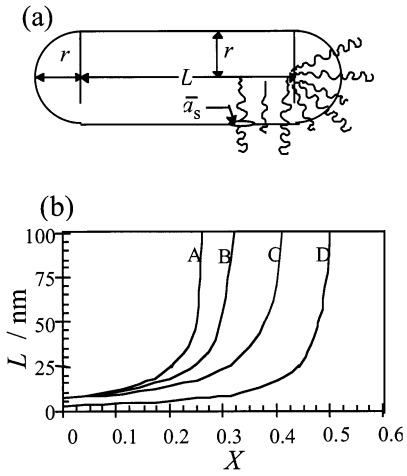

Figure 10. (a) Schematic model of a rodlike micelle. L is the cylindrical length of the rodlike lipophilic core, r and $\bar{a}_s$ are the average lipophilic length and average cross-sectional area at the hydrophilic−lipophilic interface, respectively. (b) Variation of L (calculated using eq 11) with the mole fraction of $C_{12}EO_n$ in the total amphiphile, X, for the (A) $ChEO_{10}-C_{12}EO_2$, (B) $ChEO_{10}-C_{12}EO_3$, (C) $ChEO_{10}-C_{12}EO_4$, and (D) $ChEO_{15}-C_{12}EO_3$ systems.

Discussion

The effect of the headgroup size of amphiphiles on micellar growth may be understood in terms of the mutually opposing contribution of the head and tail of amphiphiles to the interfacial curvature of the aggregate. With successive addition of $C_{12}EO_n$ molecules in the aggregate of $ChEO_m$, the hydrocarbon chain of $C_{12}EO_n$ in the aggregate increases the packing constraint in the incompressible lipophilic core of the aggregate. This effect tends to relax the packing constraint by reducing the curvature and therefore induces a sphere−rod transition if the aggregates are spherical or favors the formation of a cylindrical (less curved) interface over the highly curved (hemispherical) interface if the aggregates are already rodlike. However, headgroups of amphiphiles tend to increase the interfacial curvature depending on their size and consequently stabilize the curved interface, such as the end-caps of the rodlike aggregates. Therefore, among the amphiphiles with similar lipophilic chain lengths, the cylindrical growth of micelles is expected to be increasingly favorable with decreasing headgroup size. These contributions of the head and tail of the amphiphiles to micellar growth may be described by a simple model based on the packing of the amphiphile in the aggregate.

By considering the micellar core to be an oil pool of uniform density and composed of flexible chains and assuming the ideal mixing of amphiphiles, it is reasonable to estimate its parameters by taking the average of the contribution of each of the surfactants in the mixed system of the amphiphiles. If the structure of the rodlike micelle can be ideally expressed as in Figure 10 a, then the total volume ($\bar{V}$) and surface (A) of the mixed micelle are written in the following equations:

$$\bar{V} = \frac{4}{3}\pi r^3 + \pi r^2 L = N\bar{v} \tag{5}$$

$$A = 4\pi r^2 + 2\pi r L = N\bar{a}_s \tag{6}$$

L is the cylindrical length (excluding the hemispherical endcaps) of the rodlike micelle having a radius of cross section r (as shown in Figure 10) and composed of N amphiphilic monomers having an average interfacial cross-sectional area $\bar{a}_s$ and an average lipophilic volume $\bar{v}$. Because r is close to the hydrocarbon chain length in its extended form for spherical and rodlike micelle in the dilute region, the following approximation may be applied:

$$r = l_s \cdot X_s + l_a \cdot X_a \tag{7}$$

l is the extended chain length of an amphiphile and X is its mole fraction in the mixed system. Subscripts s and a refer to $ChEO_m$ (surfactant) and $C_{12}EO_n$ (additive), respectively. The length of the lipophilic part of $ChEO_m$, l_s, is considered to be 1.85 nm, as reported previously.[16] l_a of $C_{12}EO_n$ is taken to be 1.42 nm, the radius of a cylinder of a lipophilic core of the H_1 phase of the water−$C_{12}EO_7$ system.[27] This is a good assumption because it is known that the radius of spherical and cylindrical micelles is often close to the extended hydrocarbon chain length of amphiphiles.

At low concentrations of surfactant, the cross-sectional area, a_s, of each of the amphiphiles may be assumed to be constant. Thus, $\bar{a}_s$ and $\bar{v}$ in the mixed nonionic surfactant aggregate may be obtained from the following approximations:

$$\bar{a}_s = a_{s,s} \cdot X_s + a_{s,a} \cdot X_a \tag{8}$$

$$\bar{v} = v_s \cdot X_s + v_a \cdot X_a \tag{9}$$

v_s of $ChEO_m$ is considered to be 0.635 nm^3 from the density measurements of the $ChEO_m$ solutions.[28] The lipophilic volume v_a of $C_{12}EO_n$ may be calculated from the Tanford equations[29]

$$v \approx (27.4 + 26.9n) \times 10^{-3}\ \text{nm}^3$$

where n is the number of carbons in the hydrocarbon chain of the amphiphile. Judging from the DLS data, we considered that $ChEO_{10}$ or $ChEO_{15}$ forms short-rod micelles with the extended EO chain, as shown in Figure 10a. As a crude assumption, we consider here that the measured R_h value for the short-rod micelle is given by the sum of $0.5L$, l_s, and the EO chain length, although the relation between the cylindrical size and R_h is much more complicated. We estimate L from the available values of l_s, R_h, and the average EO chain length (taking the unit EO chain length to be ~0.20 nm in the meander configuration in aqueous solution[17]). Using values of 0.78 and 0.86 nm^2 for the

TABLE 1: Lipophilic Chain Length (l), Cross-Sectional Area at the Hydrophilic−Lipophilic Interface (a_s), and Lipophilic Volume (v) for Different Amphiphiles

	$ChEO_{15}$	$ChEO_{10}$	$C_{12}EO_4$	$C_{12}EO_3$	$C_{12}EO_2$
l/nm	1.85	1.85	1.42	1.42	1.42
a_s/nm^2	0.86	0.78	0.42	0.37	0.32
v/nm^3	0.635	0.635	0.357	0.357	0.357

average cross-sectional area of $ChEO_m$, $a_{s,s}$ for $ChEO_{10}$ and $ChEO_{15}$ micelles is obtained using eq 10, which may be derived from eqs 5 and 6. For purely spherical micelles (i.e., $L = 0$ in eq 10, which is the case of very dilute solution), we get $a_{s,s} \approx 1.0$ nm^2. This indicates that the estimated values of $a_{s,s}$ for the 0.03 M $ChEO_m$ system are not inconsistent because a_s decreases with increasing surfactant concentration in water−surfactant binary systems.

$$\bar{a}_{s,s} = \frac{3v_s(4l_s + 2L)}{4l_s^2 + 3l_sL} \tag{10}$$

$a_{s,a}$ values for $C_{12}EO_n$ are obtained from experimental results of the lamellar phase in each water−surfactant system.[18,27] The values of l, a_s, and v for each of the amphiphiles (shown in Table 1) may be substituted into eqs 7−9 to obtain variations of r, $\bar{a}_s$, and $\bar{v}$ at different X's in the mixed system. From eqs 5 and 6, we obtain

$$L = \frac{r\left(\frac{4}{3}\frac{\bar{a}_s}{\bar{v}}r - 4\right)}{2 - \frac{\bar{a}_s}{\bar{v}}r} \tag{11}$$

Then, the change in L as a function of X is calculated, and the result is shown in Figure 10b.

It can be seen that this simple calculation not only predicts small unidimensional micellar growth initially with an increasing concentration of $C_{12}EO_n$, followed by rapid growth at high $C_{12}EO_n$ content, but also shows that upon increasing the headgroup size of amphiphiles ($ChEO_m$ and $C_{12}EO_n$) micellar growth is less favored, in agreement with the results of the rheological measurements (e.g., Figure 6), although the experimental results show rapid micellar growth in 0.06 M $ChEO_{10}$−$C_{12}EO_n$ systems at a comparatively lower mixing fraction of $C_{12}EO_n$. Here, it should be noted that we used a_s values for the surfactant in the dilute region and that the data in Figure 10b can be applied only in the dilute region. With increasing surfactant concentration, a_s decreases even in a water−surfactant system. Hence, with increasing $ChEO_m$ concentration and decreasing a_s, the mixing fraction of $C_{12}EO_n$ (X) for rapid micellar growth (or viscosity) decreases, as is shown in Figure 5. Keeping this in mind, an apparent discrepancy in micellar growth indicated by the experimental results (Figure 6) and calculated data (Figure 10b) may be associated with the higher surfactant concentrations present in the systems shown in Figure 6.

The equilibrium micellar length of wormlike micelles, L, in real systems depends on several factors, for example, packing parameters of the surfactants, surfactant concentration, scission energy, and the stability of the free ends of the micelles. Equation 11 takes into account micellar growth as a function of the packing parameter only; therefore, the length L calculated from this equation gives an optimum value corresponding to the minimum in the standard chemical potential for micellization and does not represent the equilibrium length in the real system. Despite these limitations, this simple model predicts the effect of the EO chain length of $C_{12}EO_n$ on micellar growth in $ChEO_m$−$C_{12}EO_n$ systems in agreement with their rheological behavior observed in Figure 6.

Conclusions

The viscoelastic micellar phase of wormlike micelles is formed in various mixed nonionic surfactant systems, viz., aqueous $ChEO_{10}$−$C_{12}EO_n$ (n=1−4) and aqueous $ChEO_{15}$−$C_{12}EO_3$ systems in the dilute region. The phase behavior of $ChEO_{10}$−$C_{12}EO_3$−water in the dilute region shows that the highly viscous micellar phase is formed in the mixed nonionic surfactant system over a wide composition range of $ChEO_{10}$, from ∼1.5 wt % to as high as ∼15 wt %, at an appropriate mixing fraction of $C_{12}EO_3$. The increase in viscosity is attributed to the $C_{12}EO_3$-induced micellar growth leading to the formation of wormlike micelles. With increasing mixing fraction of $C_{12}EO_3$ at fixed $ChEO_{10}$ concentrations, the wormlike micelles entangle and form a viscoelastic network, as suggested by steady and oscillatory shear rheology. At high concentrations of $C_{12}EO_3$, a highly viscoelastic gel-like phase having a yield stress (∼10 Pa) and a very long relaxation time is observed. Similar rheological behavior is observed when $C_{12}EO_1$ or $C_{12}EO_2$ is used instead of $C_{12}EO_3$. With $C_{12}EO_4$, however, micellar growth is comparatively lower with respect to the concentration of additive, and no gel-like phase is formed. The ability of $C_{12}EO_n$ to induce micellar growth in $ChEO_{10}$−$C_{12}EO_n$ systems follows the order $C_{12}EO_1 \approx C_{12}EO_2 > C_{12}EO_3 \gg C_{12}EO_4$. A rapid increase in viscoelastic properties is observed with increasing concentration of $ChEO_{10}$ in the mixed surfactant system. In the 0.06 M $ChEO_{15}$−$C_{12}EO_3$ system, an increase in viscosity occurs at a relatively higher mixing ratio of $C_{12}EO_3$, but rapid micellar growth occurs with increasing concentration of $C_{12}EO_3$ and ultimately gives a viscoelastic transient network of wormlike micelles having a dynamic rheology that can be described by the Maxwellian model over a wide range of shear frequencies. Assuming that the cross-sectional area of each of the amphiphiles at the hydrophobic interface, a_s, is constant, the rod micellar length was calculated as a function of the mixing fraction of $C_{12}O_n$ in total amphiphile, X. As a result, the rod micellar length increases gradually up to a certain value of X, and above this, an enormous increase in micellar length is obtained. The effect of the headgroup size of $ChEO_m$ and $C_{12}EO_n$ on the micellar growth as predicted by the calculation is consistent with the results of rheological measurements. The micellar growth can be simply explained by decreasing the effective cross-sectional area per amphiphile in the aggregate upon addition of $C_{12}EO_n$.

Acknowledgment. D.P.A. thanks Kathmandu University, Nepal, for providing study leave.

References and Notes

(1) Kern, F.; Lemarechal, P.; Candau, S. J.; Cates, M. E. *Langmuir* **1992**, *8*, 437−440.
(2) Khatory, A.; Lequeux, F.; Kern, F.; Candau, S. J. *Langmuir* **1993**, *9*, 1456−1464.
(3) Vethamuthu, M. S.; Almgren, M.; Brown, W.; Mukhtar, E. *J. Colloid Interface Sci.* **1995**, *174*, 461−479.
(4) Kim, W.-J.; Yang, S.-M.; Kim, M. *J. Colloid Interface Sci.* **1997**, *194*, 108−119.
(5) Kim, W.-J.; Yang, S.-M. *J. Colloid Interface Sci.* **2000**, *232*, 225−234.
(6) Imai, S.; Shikata, T. *J. Colloid Interface Sci.* **2001**, *244*, 399−404.
(7) Rehage, H.; Hoffmann, H. *J. Phys. Chem.* **1988**, *92*, 4712−4719.
(8) Soltero, J. F. A., Puig, J. E.; Manero, O. *Langmuir* **1996**, *12*, 2654−2662.
(9) Raghavan, S. R.; Kaler, E. W. *Langmuir* **2001**,*17*, 300−306

(10) Montalvo, G.; Rodenas, E.; Valiente, M. *J. Colloid Interface Sci.* **2000**, *227*, 171−175.
(11) Ponton, A.; Schott, C.; Quemada, D. *Colloids Surf., A* **1998**, *145*, 37−45.
(12) Lin, Z.; Cai, J. J.; Scriven, L. E.; Davis, H. T. *J. Phys. Chem.* **1994**, *98*, 5984−5993.
(13) Kato, T.; Nozu, D. *J. Mol. Liq.* **2001**, *90*, 167−174.
(14) Seto, H.; Kato, T.; Monkenbusch, M.; Takeda, T.; Kawabata, Y.; Nagao, M.; Okuhara, D.; Imai, M.; Komura, S. *J. Phys. Chem. Solids* **1999**, *60*, 1371−1373.
(15) Kato, T.; Taguchi, N.; Nozu, D. *Prog. Colloid Polym. Sci.* **1997**, *106*, 57−60.
(16) Lopez-Quintela, M. A.; Akahane, A.; Rodriguez, C.; Kunieda, H. *J. Colloid Interface Sci.* **2002**, *247*, 186−192.
(17) Kalyanasundaram, K.; Thomas, J. K. *J. Phys. Chem.* **1976**, *80*, 1462−1473.
(18) Kunieda, H.; Umizu, G.; Yamaguchi, Y. *J. Colloid Interface Sci.* **1999**, *218*, 88−96.
(19) Cates, M. E.; Candau, S. J. *J. Phys. Condens. Matter* **1992**, *2*, 6869−6892.
(20) Menge, U.; Lang, P.; Findenegg *Colloids Surf., A* **2000**, *163*, 81−90.
(21) Wang, S.-Q.; Hu, Y.; Jamieson, A. M. In *Structure and Flow in Surfactant Solutions*; Herb, C. A., Prud'homme, R. K., Eds.; ACS Symposium Series 578. American Chemical Society: Washington, DC, 1994.
(22) Lin, Z. *Langmuir* **1996**, *12*, 1729−1737.
(23) Granek, R.; Cates, M. E. *J. Chem. Phys.* **1992**, *96*, 4758−4767.
(24) Larson, R. G. *The Structure and Rheology of Complex Fluid*; Oxford University Press: New York, 1999; Chapter 12.
(25) Kern, F.; Lequeux, F.; Zana, R.; Candau, S. J. *Langmuir* **1994**, *10*, 1714−1723.
(26) Hassan, P. A.; Candau, S. J.; Kern, F.; Manohar, C. *Langmuir* **1998**, *14*, 6025−6029.
(27) Kunieda, H.; Ozawa, K.; Huang, K. *J. Phys. Chem. B* **1998**, *102*, 831−838.
(28) Kanei, N.; Watanabe, K.; Kunieda, H. *J. Oleo Sci.*, in press.
(29) Israelahvili, J. N. *Intermolecular and Surface Forces*; Academic Press: London, 1992.